Separating monocular and binocular neural mechanisms mediating chromatic contextual interactions

Anthony D. D'Antona
Center for Perceptual Systems and Department of Psychology, University of Texas at Austin, Austin, TX, USA ✉

Jens H. Christiansen
Department of Psychology, University of Copenhagen, Copenhagen, Denmark ✉

Steven K. Shevell
Department of Psychology, University of Chicago, Chicago, IL, USA
Department of Ophthalmology and Visual Science, University of Chicago, Chicago, IL, USA
Institute for Mind and Biology, University of Chicago, Chicago, IL, USA ✉

When seen in isolation, a light that varies in chromaticity over time is perceived to oscillate in color. Perception of that same time-varying light may be altered by a surrounding light that is also temporally varying in chromaticity. The neural mechanisms that mediate these contextual interactions are the focus of this article. Observers viewed a central test stimulus that varied in chromaticity over time within a larger surround that also varied in chromaticity at the same temporal frequency. Center and surround were presented either to the same eye (monocular condition) or to opposite eyes (dichoptic condition) at the same frequency (3.125, 6.25, or 9.375 Hz). Relative phase between center and surround modulation was varied. In both the monocular and dichoptic conditions, the perceived modulation depth of the central light depended on the relative phase of the surround. A simple model implementing a linear combination of center and surround modulation fit the measurements well. At the lowest temporal frequency (3.125 Hz), the surround's influence was virtually identical for monocular and dichoptic conditions, suggesting that at this frequency, the surround's influence is mediated primarily by a binocular neural mechanism. At higher frequencies, the surround's influence was greater for the monocular condition than for the dichoptic condition, and this difference increased with temporal frequency. Our findings show that two separate neural mechanisms mediate chromatic contextual interactions: one binocular and dominant at lower temporal frequencies and the other monocular and dominant at higher temporal frequencies (6–10 Hz).

Introduction

The perceived color of a light in visual space depends on the light coming from neighboring regions (De Valois, Webster, De Valois, & Lingelbach, 1986; Shevell, 1978; Shevell & Kingdom, 2008). The same physical light may be perceived to be multiple different colors depending on the light surrounding it. The importance of context is well demonstrated when the center or surround varies over time (Christiansen, D'Antona, & Shevell, 2009; D'Antona, Kremers, & Shevell, 2011; Davey, Maddess, & Srinivasan, 1998; De Valois et al., 1986; Krauskopf, Zaidi, & Mandler, 1986; Kremers, Kozyrev, Silveira, & Kilavik, 2004; Kremers & Rimmele, 2007; Rossi & Paradiso, 1996; Shapiro, 2008; Shapiro et al., 2004; Zaidi, Yoshimi, Flanigan, & Canova, 1992). For example, if a steady central region is within a surround that is temporally varying in chromaticity, the steady central region will be perceived as temporally varying in color even though it is physically steady (Autrusseau & Shevell, 2006; De Valois et al., 1986; Krauskopf et al., 1986; Shevell & Cao, 2006). If the surround varies more rapidly than about 3 Hz, however, the induced temporal variation in the central steady region is nearly eliminated (D'Antona & Shevell, 2009; De Valois et al., 1986), though the color of the central steady region may be shifted (Christiansen et al., 2009; D'Antona & Shevell, 2006).

Contextual interactions also occur when a center region is temporally modulated and the surround is physically steady (Shapiro, 2008; Shapiro et al., 2004). If the luminance in two spatially separated central regions is temporally modulated at the same phase, and each is surrounded by the same static annulus, both central regions appear to temporally modulate together at the same phase, as expected. If, however, the static annuli surrounding the two regions region have different luminances (e.g., one appears dark and the other white), then the two central regions appear to modulate in counterphase, even though their physical temporal modulation remains identical (Shapiro, 2008; Shapiro et al., 2004). A similar effect occurs for equiluminant stimuli.

Temporally modulating both the center and surrounding regions simultaneously can produce compelling illustrations of center–surround interactions. A simple illustration of our findings for chromatic stimuli is shown in Figure 1. These stimuli can reveal the loci of neural mechanisms underlying contextual effects in perception. For example, the perceived modulation depth of a central light that is temporally varying in luminance is strongly affected by the phase of a surrounding light also varying in luminance at the same temporal frequency (D'Antona et al., 2011; Kremers et al., 2004; Kremers & Rimmele, 2007). The perceived modulation depth of the central light is described by a linear model that combines central and surrounding light stimulation. Further, the influence of the surrounding light on perceived modulation in the center results from neural mechanisms at both monocular and binocular levels (D'Antona et al., 2011). The relative contribution from mechanisms at these two levels changes with temporal frequency: The perceptual influence of the binocular mechanism is strongest at lower frequencies and attenuated above about 3 Hz, while the influence of the monocular mechanism is relatively constant for a large range of temporal frequencies (3–12 Hz).

Many properties of neurons along the visual pathway from retina to higher levels of visual cortex are well known. However, an understanding of these neural processes is incomplete without knowing how they jointly contribute to the perception or behavior of an organism. Psychophysical experiments can address this question by determining whether a given perceptual finding results from neural processing within monocular neural pathways, binocular neural pathways, or both (Barbur & Spang, 2008; D'Antona et al., 2011; D'Antona, Rosenberg, & Shevell, 2010; Flynn & Shapiro, 2013; Moutoussis & Zeki, 2000; Petrov & McKee, 2009; Shevell, Holliday, & Whittle, 1992; Shevell & Wei, 2000; Singer & D'Zmura, 1994; Webb, Dhruv, Solomon, Tailby, & Lennie, 2005). The goal of this approach is to determine the loci of the underlying neural mechanisms that contribute causally to perception.

This article investigates chromatic contextual interactions and shows that underlying neural mechanisms are within both monocular and binocular pathways. Furthermore, fits from a simple linear model combining central and surround neural responses quantitatively describe these contextual interactions. The relative magnitude and the temporal frequency tuning of these interactions show clear distinctions between the monocular and binocular levels.

Methods

Observers

Three observers participated in the study. Two were authors (ADD and JHC) and the other did not know the purpose and design of the experiments. All observers had normal color vision as determined from Rayleigh matching. Observers participated in practice sessions to become familiar with the task. The data from practice sessions were then discarded and the actual experiments were begun.

Stimuli

The stimuli were displayed on a Sony GDM-F520 cathode ray tube (CRT) color display using a Macintosh G4 computer. The display was linearized using a 10-bit lookup table. The monitor had a 1360 × 1024 pixel display and was set at a refresh rate of 75 Hz noninterlaced. The stimuli had a mean chromaticity metameric to the equal-energy spectrum (EES) and a constant luminance of 27 cd/m^2 (excluding a dark gap and fixation lines; the gap was included to separate the central and surrounding regions). All stimuli were surrounded by a thin white fixation square with two nonius crosshairs in each eye that were used to aid binocular fusion (Figure 2).

The test stimulus, which was presented in the top half of the display (Figure 2), contained a central circular patch of diameter 0.90°. The center patch was surrounded by a dark gap (inner/outer diameter of 0.90°/1.05°) and an annular surrounding field (inner/outer diameter of 1.05°/5.30°). The center and surround were presented to either the same eye (monocular condition) or opposite eyes (dichoptic condition). The fused percept was the same for both conditions (Figure 2c). The dark circular gap was always present in both eyes. The L-, M-, and S-cone excitation values were calculated using the Smith and Pokorny (1975) cone fundamentals. The center was modulated sinusoidally
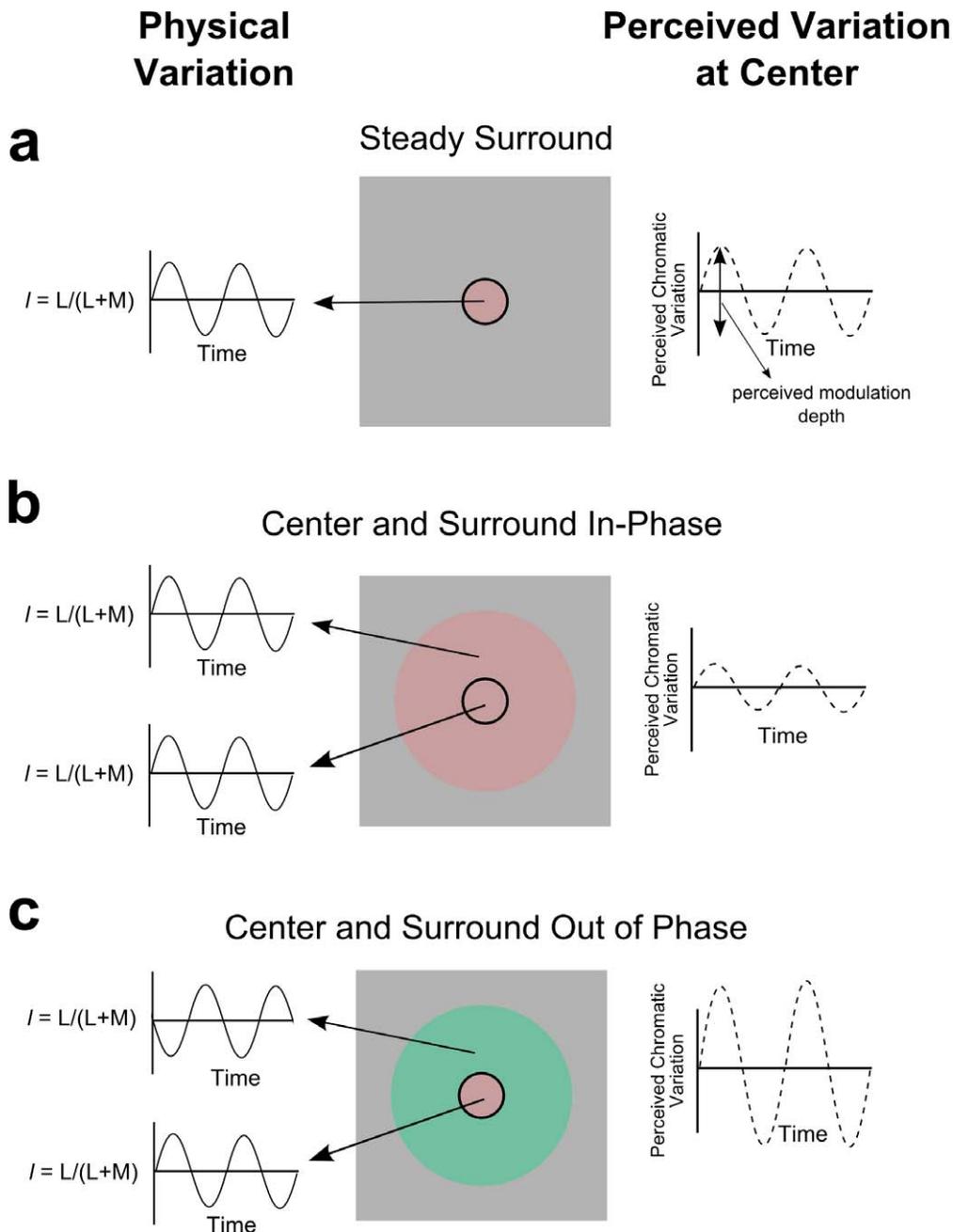
Figure 1. Basic stimulus. Physical variation is shown in the left column and perceived variation at the center is shown in the right column. (a) A circle within a dark gap was sinusoidally modulated along an L/(L + M) direction of MacLeod–Boynton color space. The perceived variation at the center is shown on the right. The difference between the perceived peak and trough of the variation is the perceived modulation depth. (b) The center and surround (separated by a dark gap) were temporally modulated at the same temporal frequency and had the same phase. The perceived variation at the center (shown at right) was reduced relative to (a). (c) The center and surround (separated by a dark gap) were temporally modulated at the same temporal frequency but in counterphase. The perceived variation at the center (shown at right) was enhanced relative to (a).

in chromaticity over time along the $l = \mathrm{L}/(\mathrm{L} + \mathrm{M})$ direction of MacLeod–Boynton chromaticity space (MacLeod & Boynton, 1979) at a Michelson contrast of 0.05 ($[l_{max} - l_{min}]/[l_{max} + l_{min}]$). The surround was also modulated sinusoidally in time at the same temporal frequency as the center and had a Michelson contrast of either 0.025 (peak and trough l values of 0.684 and 0.650, respectively) or 0.05 (peak and trough l values of 0.700 and 0.634, respectively). Center and surround frequencies always were identical and set to 3.13, 6.25, or 9.38 Hz. At the two lower frequencies, the relative phases between center and surround were −150°, −120°,
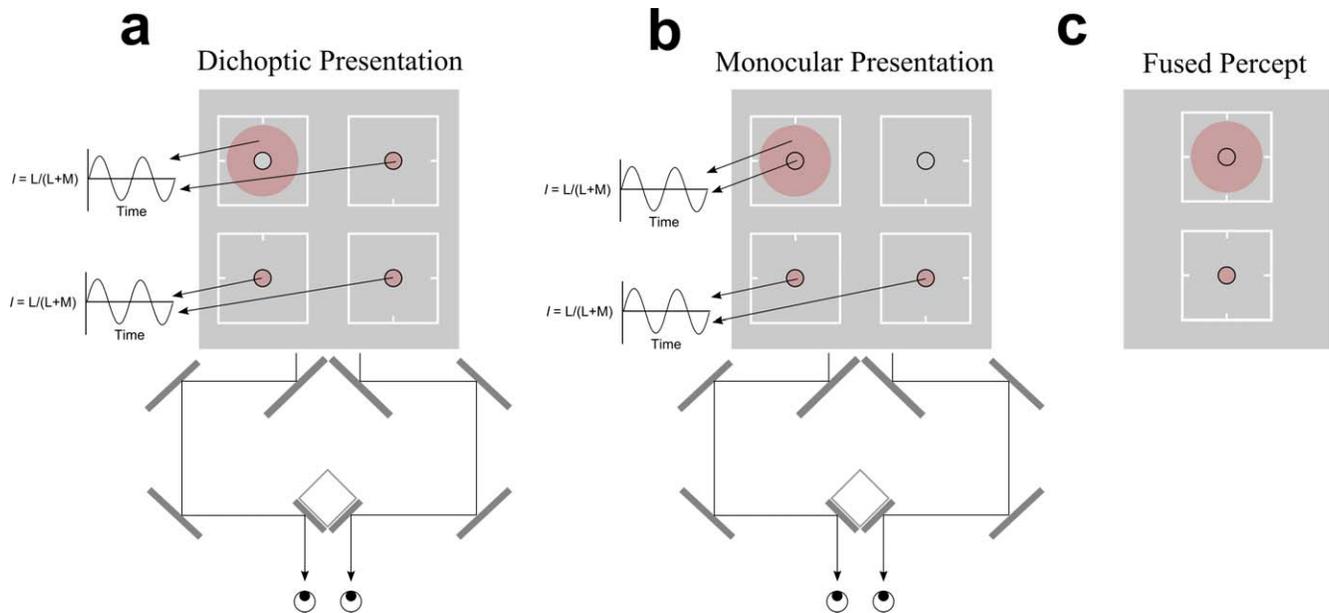
Figure 2. The experimental setup. (a) Dichoptic presentation. The test stimulus was presented on the top half of the monitor and the matching stimulus presented on the bottom half. The left and right sides of the monitor were presented to the left and right eyes, respectively, using a haploscope. In dichoptic presentation, the temporally modulating surround was presented to one eye and the temporally modulating center to the other eye. (b) Monocular presentation. Both the temporally modulating center and surround were presented to the same eye. (c) The fused percept.

$-90°$, $-60°$, $-30°$, $0°$, $30°$, $60°$, $90°$, $120°$, $150°$, and $180°$. At 9.38 Hz, the relative phases tested were $-135°$, $-90°$, $-45°$, $0°$, $45°$, $90°$, $135°$, and $180°$. Positive (negative) phase indicates that the surround's phase physically led (lagged) the center's phase.

A matching stimulus was presented in the bottom half of the display. It contained a circular field (diameter of 0.90°) surrounded by a dark gap (inner/outer diameter of 0.90°/1.05°). Its background field was steady at a chromaticity metameric to the EES and a luminance of 27 cd/m^2. The matching stimulus was modulated sinusoidally in chromaticity over time at the same temporal frequency and phase as the test-stimulus center, and was identical in both eyes (Figure 2a, b). Its modulation depth was controlled by the observer.

Procedure

Observers used a chin rest to maintain head stabilization. Heterochromatic flicker photometry was used to determine equiluminance settings for each observer. Each session started with three minutes of dark adaptation. Within a given session, monocular and dichoptic conditions for all phases were measured for a particular surround contrast level and temporal frequency. In addition, as a baseline measurement, each session included a condition with no temporal modulation within the surround. All stimuli in a given session were presented in random order and counterbalanced

for the left and right eyes. For each measurement, the observer adjusted the physical modulation depth in the matching (bottom) field to match the perceived modulation depth in the center of the test field. The observer had unlimited viewing time on each trial and was instructed to alternate fixation between the matching and test fields to determine a match. The initial modulation depth in the matching field was set randomly at the beginning of each trial. Each measurement was repeated five times within a given session, and each session was repeated on three different days. Thus, each plotted value is the average of 15 measurements.

Results

Measurements with surround Michelson contrast of 0.025 are shown in Figure 3. Each column of the figure shows results for a different observer, and each row shows measurements for a different temporal frequency. The horizontal axis of each plot represents the center–surround phase difference, and the vertical axis shows the perceived modulation depth in Michelson contrast. The blue square in each plot shows the perceived modulation depth of the central region when the surround region was physically steady. The red and green circles (solid lines) show the measurements

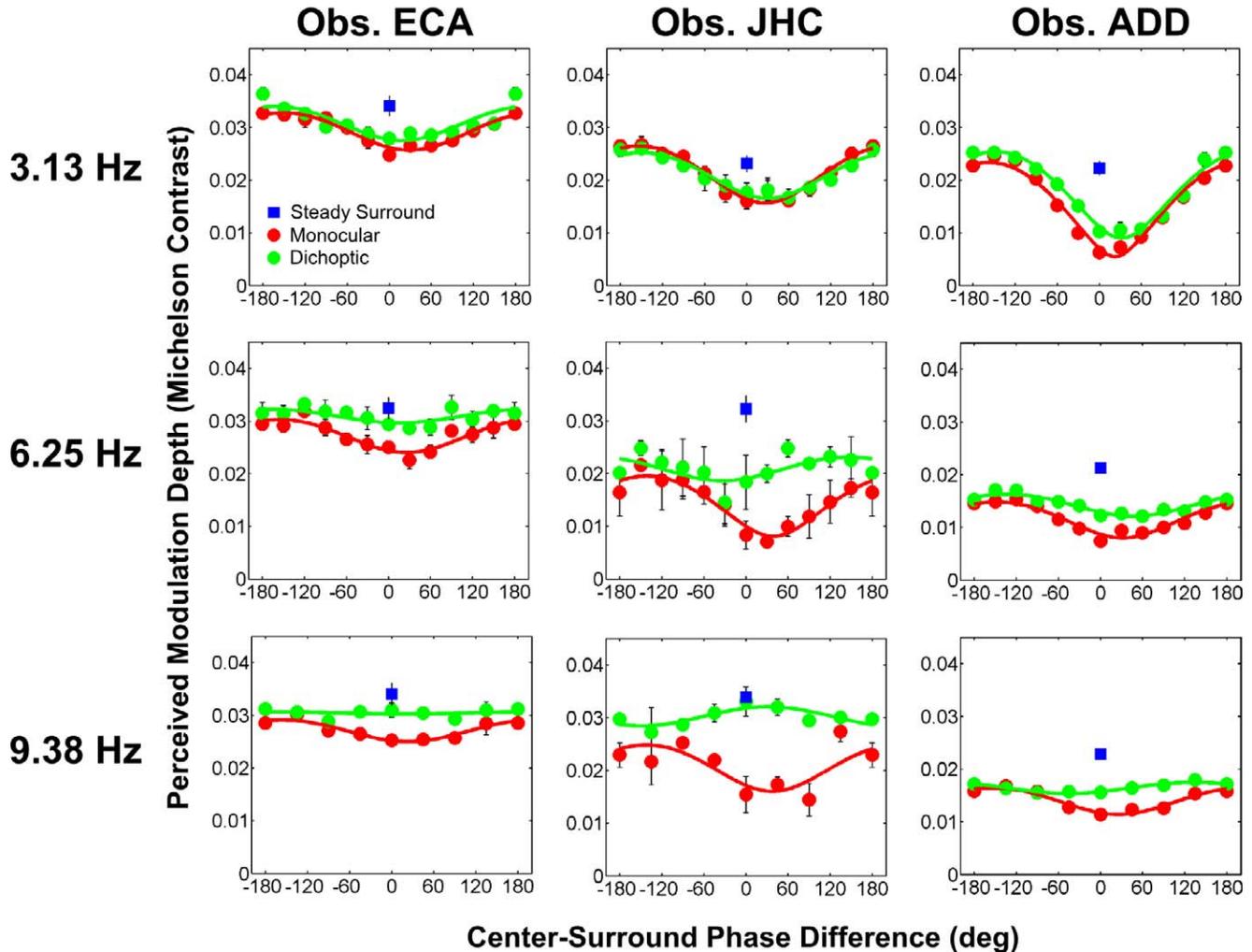# Surround Michelson Contrast = 0.025

Figure 3. Measurements with the surround modulation at 0.025 Michelson contrast. Each column shows results for one observer. The three rows show measurements for the three temporal frequencies. In each panel, the perceived modulation depth is plotted on the vertical axis, and the center–surround phase difference is on the horizontal axis. Monocular results are shown by red circles and dichoptic results by green circles. The blue square shows the perceived modulation depth with a steady surround. Lines through the plotted points are fits of the model in Equation 1 (see text). Error bars indicate one standard error of the mean.

(model fits) for the monocular and dichoptic conditions, respectively. The model is described later.

Perceived modulation depth varies as a function of the center–surround phase difference, in both the monocular and dichoptic conditions. At the lowest temporal frequency (3.13 Hz), the measurements are nearly the same for the monocular and dichoptic conditions. Thus at this temporal frequency, the lateral interactions between center and surround regions are similar regardless of whether the central and surrounding fields were presented to the same eye or different eyes. At the two higher temporal frequencies, however, the monocular and dichoptic results are distinctly different. Specifically, the dichoptic mea-

surements show less variation as a function of the center–surround phase difference than the monocular measurements. The finding that changing temporal frequency differentially influences the lateral interactions in the monocular and dichoptic conditions suggests that two distinct neural mechanisms contribute to the measurements, a point addressed later.

Another result revealed in Figure 3 is that the trough of the measurements (and model fits) does not occur at a center–surround phase difference of zero. Thus, the minimal perceived modulation depth of the center does not occur when the center and surround are physically in phase. Instead, the minimal perceived modulation depth occurs when the center–surround phase differ-
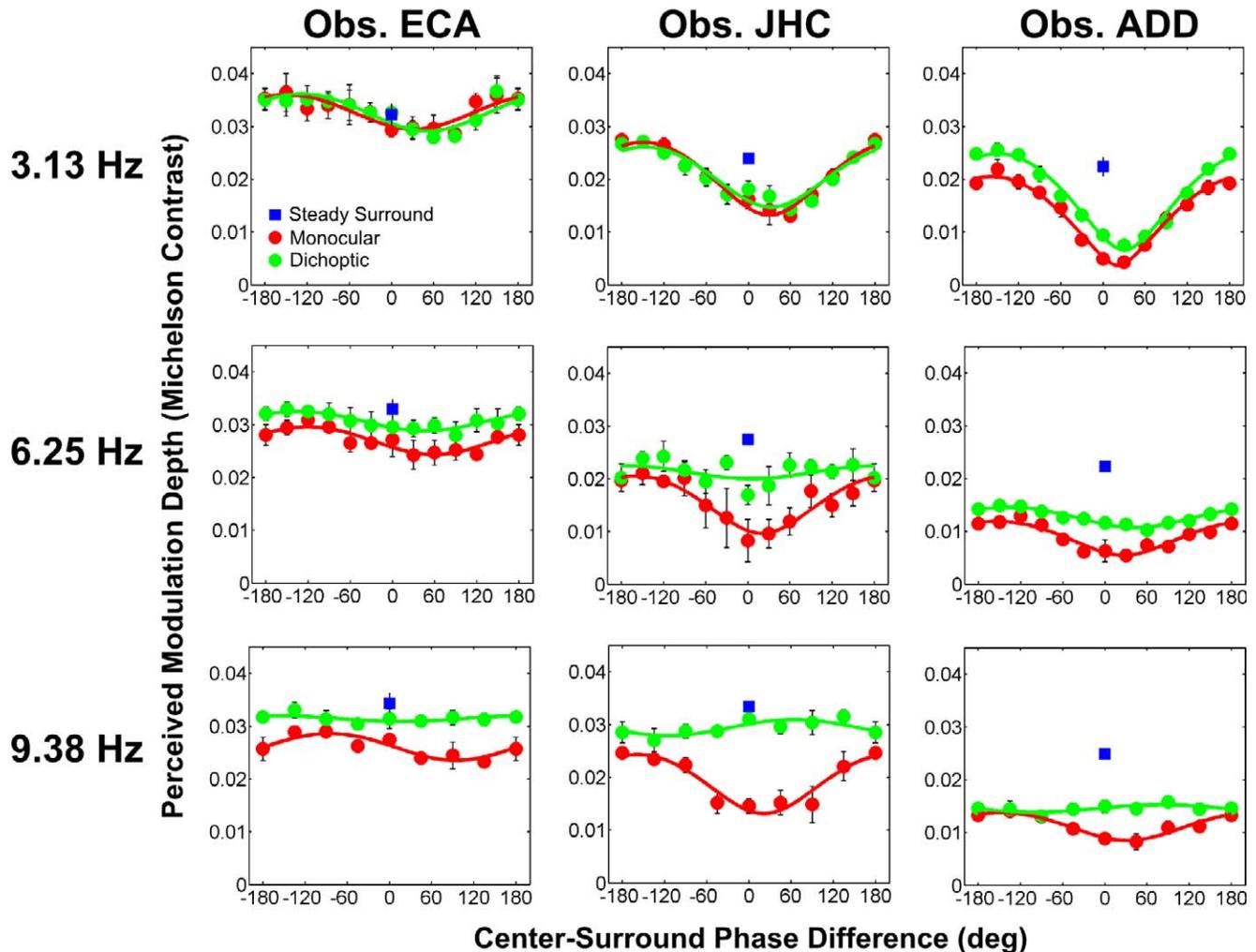
Surround Michelson Contrast = 0.05

Figure 4. As Figure 3, except with surround modulation at 0.05 Michelson contrast.

ence is greater than zero (that is, when the central modulation lags the surround modulation). This is consistent with a neural temporal lag for the surround's effect on the center.

Measurements with surround Michelson contrast of 0.05 are shown in Figure 4. All conventions are the same as in Figure 3. The same basic findings with 0.025 contrast (Figure 3) are replicated at the higher 0.05 contrast (Figure 4). At the lowest temporal frequency, monocular and dichoptic measurements are nearly identical, and this holds for each of the three observers. At higher temporal frequencies, the dichoptic measurements again show less variation as a function of center–surround phase difference than the monocular measurements. Also, the strongest suppression occurs at a center–surround phase difference greater than zero, again suggesting a neural lag for the surround. Overall, the Michelson contrast of the surround (0.025 or 0.05)

does not change the basic properties of the chromatic center–surround interactions.

Modeling

A simple model to account for perceived chromatic modulation depth uses a linear combination of central and surrounding neural responses. This model accurately describes perceived temporal *luminance* modulation (D'Antona et al., 2011; Kremers et al., 2004). Now we consider whether the same model accurately describes percepts of chromatically varying stimuli. It specifies that the amplitude of the perceived modulation depth at the center is a weighted combination of center and surround responses, with a phase shift between the central and surrounding responses. The model is conveniently represented as a vector summa-

tion. Let the central response be represented by vector $\bar{R}_C$ and the surround response by vector $\bar{R}_S$. The resultant vector $\bar{R}$ is represented as

$$\bar{R} = \bar{R}_C + \bar{R}_S, \qquad (1)$$

The vector $\bar{R}$ represents the perceived temporal variation at the center, and therefore the magnitude of $\bar{R}$ corresponds to perceived modulation depth. Applying the law of cosines, the magnitude of $\bar{R}$, denoted R, is

$$R = \sqrt{R_C^2 + R_S^2 - 2 \times R_C \times R_S \times \cos(S - \varphi)}, \qquad (2)$$

where R_C and R_S represent the magnitudes of the vectors $\bar{R}_C$ and $\bar{R}_S$, respectively. These two vector magnitudes are free parameters in Equation 2; S is the physical phase difference between center and surround; and φ, a third free parameter, represents any neural phase shift between central and surrounding responses. This model is used for all of the fits in Figures 3 and 4 and accurately describes the measurements.

The parameters from the model fits are useful for understanding the neural correlates of the observers' percepts. The quantity R_S is referred to as the surround strength and is a measure of how strongly the surround affects the response from the center. The surround strengths are plotted in Figure 5 (top row), where the horizontal axis is temporal frequency and the vertical axis is surround strength R_S. Each column shows values for a different observer. The red and green circles show monocular and dichoptic surround strengths, respectively. The solid and dashed lines are for surround Michelson contrasts of 0.025 and 0.05, respectively. These plots show that the surround strength R_S declines with increasing temporal frequency. Dichoptic surround strength decreases more steeply as a function of temporal frequency than does monocular surround strength.

The phases φ represent neural temporal phase shifts between center and surround responses. Phases are plotted in Figure 5 (bottom row). All conventions are the same as in the top row of Figure 5. While the phases show substantial variability across different observers and conditions, consistent patterns occur. Phases are relatively constant across the temporal frequencies. This result is inconsistent with a fixed time lag between central and surrounding neural responses. A fixed time lag predicts a linear increase in phase as a function of temporal frequency. Also, the phase values are much larger than in a similar previous study investigating luminance (D'Antona et al., 2011). Phase values here are in the 20°–50° range; for luminance stimuli, phase values are in the 0°–15° range.

The standard errors for the parameter estimates were calculated using a bootstrapping method. The sampling distribution of the mean for each data point was assumed to be Gaussian with a mean equal to the sample mean and standard deviation equal to the standard error. For each iteration, each data point was randomly sampled from the corresponding Gaussian distribution. After each iteration, the model was fit to the resampled data and the parameter estimates were stored. This process was repeated 5,000 times, resulting in a distribution of estimates for each parameter. The standard deviation of the distribution of the estimates for each parameter was taken to be the standard error of that parameter's estimate.

Estimating isolated monocular and binocular components

In the dichoptic condition, the influence of the surround is assumed to occur solely at a binocular level. In the monocular condition, however, the influence of the surround may occur at both a monocular level and a binocular level. Assuming additivity of the monocular and binocular effects, the perceived modulation depth in the monocular condition can be expressed by rewriting Equation 1:

$$\bar{R} = \bar{R}_C + \bar{R}_S = \bar{R}_C + \bar{R}_{S_M} + \bar{R}_{S_B}, \qquad (3)$$

where $\bar{R}_{S_M}$ and $\bar{R}_{S_B}$ represent the influences of the surround at the monocular and binocular levels, respectively (D'Antona et al., 2011). $\bar{R}_C$ and $\bar{R}_{S_B}$ can be estimated directly from the dichoptic measurements. $\bar{R}_{S_M}$ can then be estimated from the monocular-condition measurements by estimating the value of $\bar{R}_S$ and then subtracting $\bar{R}_{S_B}$.

The estimated surround strengths for the isolated monocular and binocular components are shown in Figure 6 for the three observers. The surround strengths for the isolated binocular (monocular) component for surround contrasts of 0.025 and 0.05 are shown by the green (red) circles with solid and dashed lines, respectively. The surround strengths are very similar for both surround contrast levels. The surround strength of the isolated binocular component decreases as a function of temporal frequency for all three observers, consistent with other reports of the low temporal-frequency cutoff of cortical, contextual interactions (D'Antona et al., 2011; D'Antona & Shevell, 2009; De Valois et al., 1986; Rossi & Paradiso, 1996, 1999). The surround strength of the isolated monocular component, on the other hand, is relatively flat as a function of temporal frequency for observers ECA and ADD and increases as a function of temporal frequency for JHC. This temporal frequency tuning is consistent with sensitivity to a larger range of higher temporal frequencies, as found in monocular neurons (Lee, Pokorny, Smith, & Kremers, 1994).
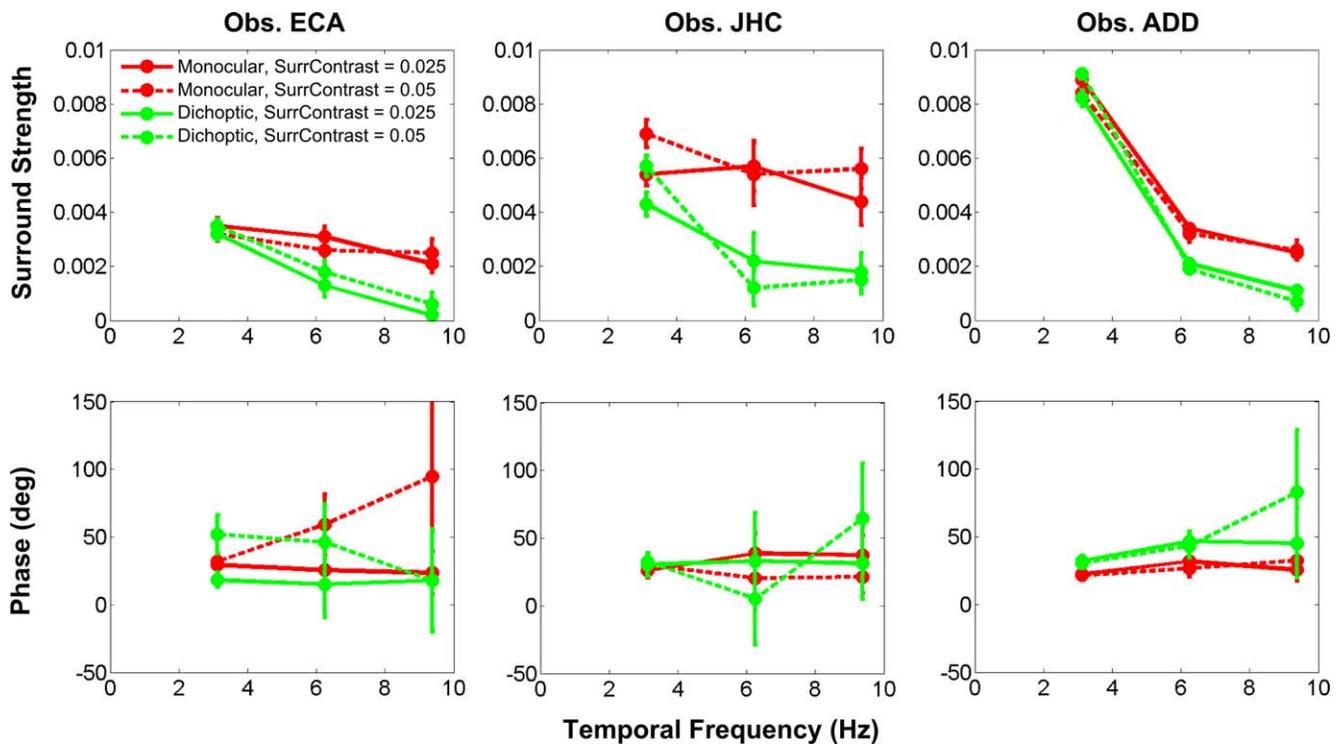
Figure 5. Parameter estimates from the model in Equation 1. Each column shows values for one observer. The two rows correspond to values for surround strength and neural phase difference, respectively. In the top row, surround strength R_S is on the vertical axis and temporal frequency is on the horizontal axis. Monocular (dichoptic) surround strengths are shown by red (green) circles, with solid and dashed lines corresponding to the 0.025 and 0.05 Michelson contrast surrounds, respectively. In the bottom row, phase shift is on the vertical axis and temporal frequency is on the horizontal axis. Symbol coding is the same as for the panels in the top row. Surround strengths and phases were estimated using Equation 2. The standard errors for each parameter estimate (shown by the vertical bars) were calculated using a bootstrapping method as described in the text.

Discussion

The percept of a central light that is temporally varying in chromaticity is strongly altered by a surrounding light that also temporally oscillates in chromaticity. In this study, central and surrounding lights modulated at the same temporal frequency, and the relative phase between center and surround was varied. Measurements of perceived modulation depth in the central field as a function of center–surround phase difference are systematic. A vector summation
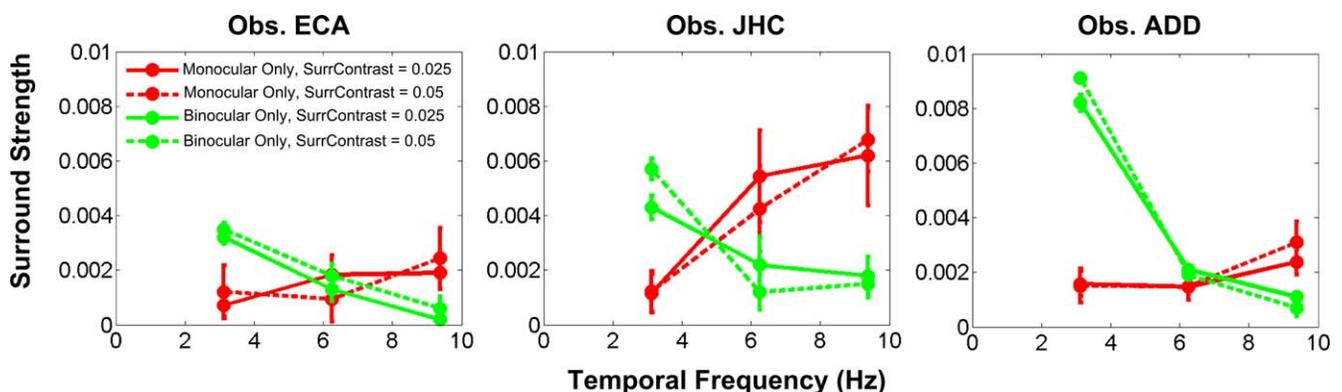

Figure 6. Estimates of isolated monocular and binocular surround strengths (see text and Equation 3), for all three observers. Surround strength is shown on the vertical axis and temporal frequency is on the horizontal axis. Estimates of isolated monocular (binocular) surround strength are shown by the red (green) circles, with the solid and dashed lines corresponding to the 0.025 and 0.05 Michelson contrast surrounds, respectively. Standard errors were again calculated using a bootstrapping technique.

model that assumes a linear combination of central and surrounding responses, along with a phase shift between center and surround responses, fits the measurements well.

The surround strengths of the contextual interactions reveal fairly low-pass temporal frequency tuning for both the monocular and dichoptic conditions, though the surround strength for the dichoptic condition is weaker and decreases more rapidly with temporal frequency compared to the monocular condition (Figure 5a). Estimated neural phase differences are positive (Figure 5b), indicating that the suppressive signal from the surround temporally lags the signal from the center. When the linear model is used to estimate the contributions to chromatic contextual interactions from isolated binocular and isolated monocular neural components, the isolated binocular component is low pass and decreases rapidly with temporal frequency, while the isolated monocular component is nearly constant or increases over the range of temporal frequencies tested (Figure 6). The low-pass tuning of the binocular component and its relatively low temporal-frequency cutoff is consistent with other studies of the temporal properties of contextual interactions presumed to be mediated by cortical mechanisms (D'Antona et al., 2011; D'Antona & Shevell, 2009; De Valois et al., 1986; Rossi & Paradiso, 1996, 1999). The faster estimated temporal tuning of the isolated monocular component is consistent with the temporal frequency tuning within monocular neural pathways (Lee, Pokorny, Smith, & Kremers, 1994).

A notable feature of the measurements in Figures 3 and 4 is that the "Steady Surround" values (blue squares) tend to have a higher perceived modulation depth compared to the other measurements. This could be due to a contrast gain-control mechanism (Heeger, 1992; Singer & D'Zmura, 1994, 1995). The chromatic temporal modulation in the surround may reduce the contrast gain in neighboring regions. If so, the modulation depth measurements of the center in the "Steady Surround" condition would be higher relative to the other measurements, since there is no surrounding modulation to reduce contrast gain.

A similar experiment was conducted in the achromatic domain (D'Antona et al., 2011). The current results with chromatic stimuli share many similarities to the findings with achromatic stimuli. First, both achromatic and chromatic stimuli show a large degree of interocular transfer. The observed lateral interactions in both the luminance and chromatic domain depend in part on binocular neural mechanisms. Second, the same simple vector summation model provides an excellent account of the measurements with both achromatic and chromatic stimuli. Third, the temporal frequency tuning for surround strength is low

pass in both the monocular and dichoptic conditions for both achromatic and chromatic stimuli. Further, when the vector summation model is used to estimate isolated monocular and binocular components, the monocular component is relatively constant as a function of temporal frequency, while the binocular component shows low-pass temporal frequency tuning.

However, several important differences exist between the achromatic and chromatic results. First, the estimates of the surround strengths for the isolated monocular and binocular components differ as a function of temporal frequency for the achromatic and chromatic domains. In the chromatic domain, the surround strength of the binocular component decreases more steeply as a function of temporal frequency, compared to the achromatic domain. Second, the phase shifts between center and surround are greater for chromatic stimuli (typically 20°–50°) compared to achromatic stimuli (generally 0°–15°). Third, at the lowest temporal frequency (about 3 Hz), the measurements for monocular and dichoptic stimuli overlap in the chromatic domain but not in the achromatic domain.

In terms of monocular neural mechanisms, contextual interactions involving achromatic and chromatic stimuli have an important difference. At a monocular level, classic neural mechanisms exist to explain lateral interactions in the achromatic domain, that is, center–surround receptive fields in the retinogeniculate pathway. These lateral interactions are antagonistic. For an on-center/off-surround cell, a light in the center will stimulate the cell, while a light presented in the surround will decrease this response.

Interestingly, no known neural mechanisms in the retinogeniculate pathway exist to implement these lateral interactions in the chromatic domain. Parvocellular receptive fields cannot account for these chromatic lateral interactions. For example, consider a +L-center/–M-surround neuron in the parvocellular pathway. A "reddish" light presented to the center excites this neuron. A "reddish" light presented in the surround modestly inhibits this response, while a "greenish" light presented in the surround inhibits the response more strongly. The results in Figures 3 and 4 show the opposite pattern: Perceived modulation depth is strongest when the chromatic center and surround are of opposite phase. At a cortical level, double opponent cells exist that do respond to chromatic contrast at edges (Conway, 2001; Conway, Hubel, & Livingstone, 2002; Johnson, Hawken, & Shapley, 2001). Our findings reveal a monocular level of chromatic interactions. One possibility is that these interactions occur in cortical double opponent cells that are monocular. An interesting experiment could determine the input from each eye to double opponent cells.

Acknowledgments

References

Autrusseau, F., & Shevell, S. K. (2006). Temporal nulling of induction from spatial patterns modulated in time. *Visual Neuroscience, 23*(3-4), 479–482.

Barbur, J. L., & Spang, K. (2008). Colour constancy and conscious perception of changes of illuminant. *Neuropscyhologia, 46,* 853–863.

Christiansen, J. H., D'Antona, A. D., & Shevell, S. K. (2009). The neural pathways mediating color shifts induced by temporally varying light. *Journal of Vision, 9*(5):26, 1–10, http://www.journalofvision.org/content/9/5/26, doi:10.1167/9.5.26. [PubMed] [Article]

Conway, B. R. (2001). Spatial structure of cone inputs to color cells in alert macaque primary visual cortex (V-1). *Journal of Neuroscience, 21*(8), 2768–2783.

Conway, B. R., Hubel, D. H., & Livingstone, M. (2002). Color contrast in macaque V1. *Cerebral Cortex, 12,* 915–925.

D'Antona, A. D., Kremers, J., & Shevell, S. K. (2011). Perceived temporal variation due to context: Contributions from two distinct neural mechanisms. *Vision Research, 51,* 1853–1860.

D'Antona, A. D., Rosenberg, A. R., & Shevell, S. (2010). The neural locus underlying perception of the Craik–O'Brien–Cornsweet Effect. [Abstract]. *Journal of Vision, 10*(7): 416, http://www.journalofvision.org/content/10/7/416, doi:10.1167/10.7.416. [Abstract]

D'Antona, A. D., & Shevell, S. K. (2006). Induced steady color shifts from temporally varying surrounds. *Visual Neuroscience, 23,* 483–487.

D'Antona, A. D., & Shevell, S. K. (2009). Induced temporal variation at frequencies not present in the stimulus: Evidence for a neural nonlinearity.

Journal of Vision, 9(3):12, 1–11, http://www.journalofvision.org/content/9/3/12, doi:10.1167/9.3.12. [PubMed] [Article]

Davey, M. P., Maddess, T., & Srinivasan, M. V. (1998). The spatiotemporal properties of the Craik–O'Brien–Cornsweet effect are consistent with "filling-in." *Vision Research, 38*(13), 2037–2046.

De Valois, R. L., Webster, M. A., De Valois, K. K., & Lingelbach, B. (1986). Temporal properties of brightness and color induction. *Vision Research, 26*(6), 887–897.

Flynn, O. J., & Shapiro, A. G. (2013). The separation of monocular and binocular contrast. *Vision Research, 93,* 19–28.

Heeger, D. J. (1992). Normalization of cell responses in cat striate cortex. *Visual Neuroscience, 9,* 181–197.

Johnson, E. N., Hawken, M. J., & Shapley, R. (2001). The spatial transformation of color in the primary visual cortex of the macaque monkey. *Nature Neuroscience, 10*(9), 1185–1190.

Krauskopf, J., Zaidi, Q., & Mandler, M. B. (1986). Mechanisms of simultaneous color induction. *Journal of the Optical Society of America A, 3*(10), 1752–1757.

Kremers, J., Kozyrev, V., Silveira, L. C. L., & Kilavik, B. E. (2004). Lateral interactions in the perception of flicker and in the physiology of the lateral geniculate nucleus. *Journal of Vision, 4*(7):10, 643–663, http://www.journalofvision.org/content/4/7/10, doi:10.1167/4.7.10. [PubMed] [Article]

Kremers, J., & Rimmele, U. (2007). The spatial extent of lateral interactions in flicker perception. *Vision Research, 47,* 16–21.

Lee, B. B., Pokorny, J., Smith, V. C., & Kremers, J. (1994). Responses to pulses and sinusoids in macaque ganglion cells. *Vision Research, 34*(23), 3081–3096.

MacLeod, D. I., & Boynton, R. M. (1979). Chromaticity diagram showing cone excitation by stimuli of equal luminance. *Journal of the Optical Society of America A, 69,* 1183–1186.

Moutoussis, K., & Zeki, S. (2000). A psychophysical dissection of the brain sites involved in color-generating comparisons. *Proceedings of the National Academy of Sciences, USA, 97*(14), 8069–8074.

Petrov, Y., & McKee, S. P. (2009). The time course of contrast masking reveals two distinct mechanisms of human surround suppression. *Journal of Vision, 9*(1):21, 1–11, http://www.journalofvision.org/content/9/1/21, doi:10.1167/9.1.21. [PubMed] [Article]

Rossi, A. F., & Paradiso, M. A. (1996). Temporal limits

of brightness induction and mechanisms of brightness perception. *Vision Research, 36,* 1391–1398.

Rossi, A. F., & Paradiso, M. A. (1999). Neural correlates of perceived brightness in the retina, lateral geniculate nucleus, and striate cortex. *Journal of Neuroscience, 19*(14), 6145–6156.

Shapiro, A. G. (2008). Separating color from color contrast. *Journal of Vision, 8*(1):8, 1–18, http://www.journalofvision.org/content/8/1/8, doi:10.1167/8.1.8. [PubMed] [Article]

Shapiro, A. G., D'Antona, A. D., Charles, J. P., Belano, L. A., Smith, J. B., & Shear-Heyman, M. (2004). Induced contrast asynchronies. *Journal of Vision, 4*(6):5, 459–468, http://www.journalofvision.org/content/4/6/5, doi:10.1167/4.6.5. [PubMed] [Article]

Shevell, S. K. (1978). The dual role of chromatic backgrounds in color perception. *Vision Research, 18,* 1649–1661.

Shevell, S. K., & Cao, D. (2006). Chromatic assimilation measured by temporal nulling. *Vision Research, 46*(1-2), 106–116.

Shevell, S. K., Holliday, I., & Whittle, P. (1992). Two separate neural mechanisms of brightness induction. *Vision Research, 32*(12), 2331–2340.

Shevell, S. K., & Kingdom, F. A. (2008). Color in complex scenes. *Annual Review of Psychology, 59*, 143–166.

Shevell, S. K., & Wei, J. (2000). A central mechanism of chromatic contrast. *Vision Research, 40,* 3173–3180.

Singer, B., & D'Zmura, M. (1994). Color contrast induction. *Vision Research, 34*(23), 3111–3126.

Singer, B., & D'Zmura, M. (1995). Contrast gain control: A bilinear model for chromatic selectivity. *Journal of the Optical Society of America A, 12*(4), 667–685.

Smith, V. C., & Pokorny, J. (1975). Spectral sensitivity of the foveal cone photopigments between 400 and 500 nm. *Vision Research, 41*, 1007–1021.

Webb, B. S., Dhruv, N. T., Solomon, S. G., Tailby, C., & Lennie, P. (2005). Early and late mechanisms of surround suppression in striate cortex of macaque. *Journal of Neuroscience, 25*(50), 11666–11675.

Zaidi, Q., Yoshimi, B., Flanigan, N., & Canova, A. (1992). Lateral interactions within color mechanisms in simultaneous induced contrast. *Vision Research, 32*(9), 1695–1707.